Sox9^{+} Cell is Required for Salivary Gland Regeneration after Radiation Damage via Wnt/β-Catenin Pathway

Xiuyun Xu
Sun Yat-Sen University Guanghua School of Stomatology
Xiong Gan
Sun Yat-Sen University Guanghua School of Stomatology
Ming Zhang
Sun Yat-Sen University Guanghua School of Stomatology
Jiaxiang Xie
Sun Yat-Sen University Guanghua School of Stomatology
Shuang Chen
Sun Yat-sen University First Affiliated Hospital
Jingting Li
Sun Yat-sen University First Affiliated Hospital
Yong Bao
Sun Yat-sen University First Affiliated Hospital
Cheng Wang
Sun Yat-Sen University Guanghua School of Stomatology
Demeng Chen (chendm29@mail.sysu.edu.cn)
Sun Yat-sen University First Affiliated Hospital https://orcid.org/0000-0001-7230-2495

Research Article

Keywords: Radiation induced salivary gland injury, Sox9, Wnt/β-catenin pathway, regeneration, organoids

Posted Date: May 27th, 2021

DOI: https://doi.org/10.21203/rs.3.rs-535738/v1

Abstract

Background**:** Radiotherapy for head and neck cancer can cause serious side effects, including severe damage to the salivary glands, resulting in symptoms such as xerostomia, dental caries, oral infectious and so on. Due to lack of long-term treatment for the symptoms of saliva barren, current research has focused on finding endogenous stem cells that can differentiate into various cell lineage to replace lost tissue and restore function.

Results: In our study, we identified $Sox9^+$ cells can differentiate into various salivary epithelial cell lineages under homeostatic conditions. After ablating $Sox9^+$ cells, the salivary glands of irradiated mice showed more severe phenotypes and reduced proliferative capacity. Analysis of online single cell RNA-sequencing data revealed enrichment of the Wnt/β-catenin pathway in $Sox9^+$ cell population. Furthermore, treatment of Wnt/β-catenin inhibitor to irradiated mice inhibited the regenerative capability of $Sox9^+$ cells. Finally, we showed that $Sox9^+$ cells were able to form organoids in vitro and transplanting these organoids into salivary glands after radiation restored part of salivary gland function.

Conclusions**:** In short, our research indicated that regenerative therapy targeting $Sox9^+$ cells is a promising method to solve the radiation induced salivary gland injury.

Background

Head and neck cancer is the sixth most common cancer worldwide, with over 600,000 cases and around 300,000 deaths per year(1) .At present, surgical removal of the primary tumor is mainly used for head and neck cancer, combined with radiotherapy and chemotherapy. Unfortunately, radiotherapy of the head and neck inevitably leads to organic damage and dysfunction of the salivary glands including dry mouth, tooth decay, oral infection, and impaired taste and speech, seriously affecting the patient's quality of life(2). The current treatment methods for radiation-induced salivary gland damage mainly depend on short-term relief from the symptoms, such as commercial saliva substitutes, but short of long-term restorative therapies.

In clinical practice, radiotherapy may damage other organs, including lungs, heart, bladder(3), but there are few, if any, options available to restore lost tissue. Recently, emerging studies about radiation-induced damage concentrate on regenerative strategies such as stimulating the potential of endogenous stem cells or transplanting non-irradiated stem cells(4–6). However, the identification of stem cells under homeostatic or injury conditions is a roadblock in the application of regeneration strategies. Although recent studies have shown that acinar cells are derived through self-duplication following duct ligation injury, their cell subpopulation have not been confirmed(7). It is significant to identify whether the regeneration of acinar under radiation damage is self-duplication or derived from stem cells.

Over the last several years, the use of genetic lineage tracing to map fate of stem cells revealed the dynamics of cell fate-specific patterns during development, tissue maintenance and repair(8). Salivary

glands are composed of four main lineages, including the acinar, ductal, myoepithelial and basal cells. Prior studies have demonstrated that the basal and myoepithelial cell populations widely expressing keratin 14 (K14) and keratin 5(K5) function as multipotent stem cells and contribute to all epithelial cell lineages during development(9, 10). However, in adult salivary gland, $K14^+$ cells remained lineage restricted and lost differentiation potential(11, 12). Lineage tracing experiments confirmed that the sex-determining Region Y (SRY) box (Sox) family members Sox9 contributes to acinar and ductal cells during the salivary gland development(13). However, in adult salivary glands, whether $Sox9^+$ cells can remain lineage restrict and maintain the subpopulation of acinar cells under homeostatic or injury conditions remains unknown.

In this study, we performed in vivo genetic lineage tracing experiments in the mouse submandibular gland and unexpectedly discover that $Sox9^+$ cells have the ability of repopulating lost functional compartment after radiation-induced damage. Analysis of single-cell RNA-sequencing (scRNA-seq) online dataset of salivary gland, show that Wnt/β-catenin pathway was enriched in cells with high Sox9 expression. Using inhibitor to block the Wnt/β-catenin pathway has indeed suppressed the repair and regeneration ability of the salivary glands. In addition, an emerging three-dimension organoid culture method that can recapitulate the structure, functionality and genetic characteristics of the original tissues has been established as an important tool for many basic biological applications, such as organoid transplantation(14). We transplanted $Sox9^+$ cells into the submandibular glands of mice injured by radiation and found that successfully transplanted organoids can substitute part of the damaged salivary gland tissue. To sum up, our data revealed the extensive regenerative capacity of $Sox9^+$ cells in salivary glands and suggested that $Sox9^+$ organoid may be an effective treatment of radiation-damaged salivary glands.

Results

$Sox9^+$ cells mainly generate acinar cells in the SMG under homeostatic conditions

To characterize the expression of Sox9 in the salivary glands of adult mice, we first performed immunohistochemical (IHC) staining on salivary gland tissues of normal mice at different anatomic sites. We found presence of Sox9 protein in all three major paired (parotid, submaxillary and sublingual) salivary glands (Fig. 1A). However, we detected no positive signal of Sox9 IHC staining in the minor salivary glands (Fig. 1B), suggesting possible different roles of Sox9 in salivary glands at different anatomic sites. Because submandibular gland (SMG) is the largest salivary secreting organ in mice, we then used SMG for our following study. $Sox9^+$ cells have been shown to be a progenitor population that can produce acinar and ducts during embryonic developmental stage [15]. However, their roles in adult murine salivary gland remain unknown. To investigate that, we injected a single of tamoxifen to adult *Sox9creER*; *Rosa-tdTomato* mouse and traced $Sox9^+$ cells for different periods of time under homeostatic conditions (Fig. 1C). Two days after the initial tamoxifen administration, we found that $Tomato^+$ cells were mainly overlapped with the $Aqp5^+$ acinar cells, but not in the $Krt18^+$ ductal cells, $Acta2^+$

myoepithelial cells or Krt14$^+$ basal cells (Fig. 1D). After 7 days, we detected expansion of Tomato$^+$ clones in acinar cell compartment (Fig. 1D). Notably, Tomato$^+$ cells were observed in different cell lineages, including Aqp5$^+$ acinar cells, Krt18$^+$ ductal cells, Acta2$^+$ myoepithelial cells and Krt14$^+$ basal cells 30 days after initial injection of tamoxifen (Fig. 1D). 90 days after tracing, we found an increased number of Aqp5$^+$/Tomato$^+$ double positive cells (58.75% ± 3.59%) Acta2$^+$/Tomato$^+$ (2.03% ± 0.81%), Krt14$^+$/Tomato$^+$(3.64% ± 0.48%)as well as Krt18$^+$/Tomato$^+$ 4.25% ± 0.9% double positive cells in the SMG tissues (Fig. 1D, E). Overall, our genetic lineage tracing studies demonstrated that Sox9$^+$ cells function as multipotent cells contributing to all epithelial cell lineages under homeostatic conditions, and produce most part of acinar cells in these cell types.

Sox9$^+$ cells are required for radiation-induced regeneration of SMG

To study the role of Sox9$^+$ cells in the wound-healing process of salivary gland, we generated *Sox9creER, Rosa-tdTomato*, *Rosa26-DTA* mice, which allow us to specifically ablate Sox9$^+$ cells upon tamoxifen administration. Our results demonstrated that Sox9$^+$ cells underwent cell death as a result of diphtheria toxin A chain (DTA) expression (Fig. 2A, 2E). We then perform a functional evaluation of the salivary gland after radiation exposure and found that there is a significant decrease in saliva secretion in the *Sox9creER*, *Rosa-tdTomato*, *Rosa26-DTA* compared with control *Sox9creER, Rosa-tdTomato* mice after a month (Fig. 2B). Furthermore, H&E and Masson's Trichrome staining also revealed that the experimental group suffered more severe morphological damage, such as massive destruction of acinar cells, and wider range of fibrosis than the control group after radiation (Fig. 2C, 2D). Results from TUNEL assay and Ki67 IHC staining indicated that ablating Sox9$^+$ cells of SMG caused highly apoptosis and lower proliferation in SMG tissue (Fig. 2F, 2G). Moreover, compared to control group, the SMG in *Sox9creER, Rosa-tdTomato, Rosa26-DTA* displayed a greater loss of acinar cells and ductal cells and higher degree of tissue architectural disruption (Fig. 3A, 3C). 90 days after tracing, we found about 47.55% ± 3.18% Aqp5$^+$/ Tomato$^+$ double positive cells than the control group (Fig. 3B). Surprisingly, Krt18$^+$/Tomato$^+$(11.7% ± 1.27%)double positive cells increased dramatically compared with homeostatic conditions in the SMG tissues (Fig. 3D).In summary, Sox9$^+$ cells play a critical role during regeneration and repair process of SMG after radiation injury.

scRNA-seq analysis revealed activation of Wnt/β-catenin pathway in Sox9$^+$ cells

To investigate the possible mechanism in regulating Sox9$^+$ SMG cells, online single-cell RNA-sequencing (scRNA-seq) datasets regarding cell populations involved in salivary gland development and maintenance was downloaded and analyzed. Since our study mainly focused on the adult salivary gland tissue, we only utilized the dataset generated using adult mouse. We clustered cells from online dataset into six different categories, including acinar cells, basal cells, ductal cells, endothelial cells, monocytes and myoepithelial cells (Fig. 4A). Subsequently, we extracted acinar cells and reclustered them into Sox9$^+$

cells and $Sox9^-$ cells population according to the Sox9 expression level (Fig. 4B). Although cell cycle analysis showed no significant difference between these two populations (Fig. 4C), KEGG enrichment analysis showed several pathways, including Wnt/β-catenin pathway, cytokine receptor interaction and extracellular matrix receptor interaction, were significantly enriched in $Sox9^+$ cells (Fig. 4D). Since intensive studies have support a critical role Wnt/β-catenin pathway in the regulation of the stem cell fate and adult tissue regeneration(15), we postulated it might take part in the regulation of $Sox9^+$ SMG cells. We then examined the Wnt/β-catenin pathway targets Ccnd1, Tbx4 and found that they overlap with $Sox9^+$ cells population (Fig. 4E). In conclusion, the results of single-cell sequencing analysis indicated that the Wnt/β-catenin pathway might be important in the maintenance of $Sox9^+$ cell population.

Wnt/β-catenin pathway inhibitors aggravate salivary gland radiation damage

To test whether blocking Wnt/β-catenin pathway can affect the regenerative capacity of $Sox9^+$ cells in salivary gland, a highly effective inhibitor (XAV-939) of Wnt/β-catenin pathway was applied (Fig. 5A). Saliva flow examination of the SMG exhibited a substantial decline in the XAV-939 treated group (Fig. 5B). Histological analysis showed that the submandibular gland displayed large areas of acini loss and more serious fibrosis after treatment of XAV-939 (Fig. 5C, D). Lineage tracing results revealed smaller $Sox9^+$ clones were formed after treatment of XAV-939, indicated regenerative ability compromised (Fig. 5E). The ability to proliferate of the salivary gland epithelium is also greatly reduced (Fig. 5F, G). In addition, the cell apoptotic rate was higher in the treatment group compared with the controls (Fig. 5H, I). Thus, our data indicated that Wnt/β-catenin pathway is essential for the regenerative capacity of $Sox9^+$ cells.

Transplant of $Sox9^+$ organoids improved the regeneration of damaged salivary glands

To test whether $Sox9^+$ cells are able to form organoid in vitro, we isolated $Tomato^+$ cells from SMG. In the culture conditions, salivary gland organoids models derived from *Sox9creER*; *Rosa-tdTomato* mouse typically developed within 4 weeks (Fig. 6A). Organoids showing strong tomato signal also displayed different forms, either a cystic or a lumen-like phenotype (Fig. 6B). The organoids retained characteristic of differentiated salivary gland by immunostaining for the classical markers, including Aqp5, Krt18, Acta2 and Krt14 (Fig. 6C). To test whether these organoids were able to regenerate mouse salivary glands, we collected about 200 organoids and injected them into wild-type mice submandibular gland that suffered from radiation damage. Then, we indeed observed that tomato signal appeared in submandibular glands and distributed in the acinar and duct (Fig. 6D). What's more, the function evaluation experiment of salivary glands also showed the positive effect of transplanting $Sox9^+$ organoids (Fig. 6E). The above data implies that $Sox9^+$ organoid can be expanded in vitro and supplement salivary gland cells damaged by radiation.

Discussion

Most patients suffering from head and neck cancer requires radiation therapy in combination with other treatment, including surgical resection, radiotherapy and chemotherapy(16). However, radiotherapy around the head and neck will inevitably destroy salivary glands, resulting in impairment of saliva secretion and decline in quality of life. Our study using a murine model to characterize repair and regeneration revealed that $Sox9^+$ cells as progenitors in the adult salivary gland was essential to the replenishment of acinar and ductal cells after radiation-induced damage. Hence, our study provides some insights for the feasibility of using stem cells to treat damaged salivary glands.

Over the last several years, effort has been made to identify stem/progenitor cell in salivary gland. Studies have shown that these cell populations have an impact on all aspects of salivary gland biology, including cell fate specification during development, adult tissue regeneration and the role of stem cell in carcinogenesis(8). Previous research discovered that $Sox9^+$ cells played an essential role as a biomarker for progenitor multipotent progenitor cells in the developing pancreas, mammary gland, lung, liver and duodenum(17–22). To explore the role of $Sox9^+$ cells in adult salivary gland, by labeling $Sox9^+$ cells, we monitored the cell fate trajectory and find that $Sox9^+$ cells contribute all cell lineages of salivary gland under homeostatic conditions. We further investigated that mice with ablation of $Sox9^+$ cells using diphtheria toxin A chain (DTA) show more severe phenotype including structural destruction, increased apoptosis and severe fibrosis, compared with control groups. What's more, the study unexpectedly showed that $Sox9^+$ cells can differentiate into acinar cells and ductal cells after injury. In contrast to Aure and co-workers' report showing that acinar cells replenish through self-duplication of mature cells(7), our result confirmed that $Sox9^+$ cells serving as a progenitor maintain both the acinar and ductal cell lineages.

Using the prevailing single-cell sequencing method, KEGG enrichment analysis discovered Wnt/β-catenin pathway, which is closely related to cell differentiation. $Sox9^+$ cells can be used as progenitor cells to differentiate into various types of cells so as to restore missing structure. And our application of Wnt/β-catenin pathway inhibitors has also proved that blocking this pathway will make it difficult for the injured salivary glands to be repaired and then behave more serious phenotype.

Recently, many studies designed to exploit the potential of stem cell population to regenerate the missing radiation damage cell structures(23, 24). Organoid technology, as an emerging independent tool, offer enormous possibilities for the basic research on tissue development, stem cell characteristics(25), regeneration medicine etc.(26, 27). Studies have shown that intestinal stem cell organoid transplantation can restore the function of the intestinal mucosa and treat bile acid malabsorption in rats(28). Our experiment used the model to reconstruct the damaged structure and achieved good results. However, we also found that the organoids did not proliferate in the salivary glands one month after transplantation, which may be due to the insufficient recovery time. Anyway, the method, organoids transplantation, provides a good idea for the subsequent treatment of salivary gland radiation damage.

Conclusion

Taken together, our data highlight Sox9^{+}cells in the salivary gland, as a progenitor cell population, can occurs the expansion and differentiation capacity through Wnt/β-catenin pathway. Combined organoid transplantation can effectively restore the function of damaged salivary glands. Based on the above research, targeting Sox9^{+} cells have potential therapeutic benefits against radiation-damaged salivary glands.

Methods

Mouse lines

All animal experiments and procedures were approved by sun yat-sen University Institutional Animal Care and Use Committee (IACUC) and complied with the guidelines for the use and care of laboratory animals. *Sox9creER, Rosa-tdTomato* and *Rosa-DTA* mice were purchase from the Jackson Laboratory.

Lineage tracing experiment

6-8week old adult *Sox9creER, Rosa-tdTomato* mice received tamoxifen (Sigma, T5648-1G) dissolved in corn oil by intraperitoneal injection with dose of 0.08 mg/g body weight every day for three consecutive days. Mice were anesthetized by 1% pentobarbital with 0.05mg/g body weight and submandibular glands were harvested at 1st day, 1st week, 1st month, 2nd months, and 3rd months post-injection. To exclude sexual dimorphism of murine salivary glands, all experiments in this study were performed in both sexes.

Radiation-induced damage experiment

Sox9creER, Rosa-tdTomato mice and *Sox9creER, Rosa-tdTomato* and *Rosa-DTA* mice were anesthetized before irradiation. They were placed in a radiation protection lead box and only exposed neck and part of the head. Each mouse received a single dose of 15Gy from a Cs137 gamma radiation source (Rs2000, USA). All mice were given soft diet and clear water after recovery from anesthesia. Their submandibular glands were harvested at 1st,7th,15th,30th,60th and 90th. For Wnt/β-catenin pathway inhibitor treatment, each irradiated *Sox9creER, Rosa-tdTomato* mice were intraperitoneally injected with Wnt/β-catenin pathway inhibitor (XAV-939 5ul/g) (X3004-5MG, Sigma-Aldrich) for five consecutive days. The control group was injected with corn oil at the same time. These submandibular gland samples were collected at 1st, 3rd, 7th, 15th, 30th, 60th, 90th.

Saliva collection and analysis

All mice were intraperitoneally injected with 1% pentobarbital with 0.05mg/g body weight to keep the mouse still. About two minutes later, pilocarpine (0.5mg/kg i.p.) was injected into their bodies by intraperitoneal injection. Fifteen minutes later, saliva was collected via cotton ball in pre-weighed Ep tubes. 1mg saliva can be calculated as 1ul. Finally calculate the salivary gland flow rate(ul/min).

Tissue processing

The submandibular gland samples were fixed in 4% paraformaldehyde (biosharp, BL539A) at 4°C overnight. After fixation, salivary glands were processed for OCT and paraffin embedding. 8-um frozen sections were cut and store at -20°C. 5um paraffin sections were cut using a microtome (Leica) and stored at room temperature.

Hematoxylin and Eosin Staining and Masson's trichrome staining

After deparaffinization and hydration, paraffin sections were stained with hematoxylin and eosin according to standard protocol (Solarbio, G1120-100). Masson's trichrome staining was performed following the standard protocol (G1343, Solarbio). Then carry out ethanol dehydration and neutral resin sealing.

Immunohistochemical staining

For immunohistochemical studies, 5 um paraffin sections were deparaffinized and rehydrated. They are incubated in a 3% hydrogen peroxide solution for 10 minutes to remove endogenous peroxidase activity. Then antigen retrieval was performed with sodium citrate buffer (pH 6.0) using Microwave oven. After incubating in peroxide blocking buffe (BSA) for 30 minutes in 37°C thermostat, sections were incubated with rabbit monoclonal anti-Sox9 antibody (1:200, CST, 82630S) at 4°C overnight, followed by 1 hour incubation with the goat anti-rabbit kit (SA1022, BOSTER). Finally, use DAB (AR1022, BOSTER) to develop the color under the microscope. For peroxidase reactions, color was developed for 5 mins in DAB solution and counterstained with hematoxylin for1 minute.

Immunofluorescence staining and TUNEL staining

Frozen sections were fixed in 4% paraformaldehyde for 10 minutes at room temperature. Then, the slides were circled with a PAP pen and blocked in 5% BSA, 0.1% TritonX-100 and 10%NDS in PBS for 1 hour after washed three times with PBS. The tissues were incubated with primary antibodies overnight at 4℃; alpha-smooth muscle actin (SMA) (1:200, BM0002, BOSTER), K14 (1:500, ab7880, Abcam), K18(1:500, bsm-33101M, Bioss), Ki67 (1:1000; Proteintech, 27309), Aqp5 (1:1000, AB3559, Millipore). The following day, sections were rinsed in PBS dilution and then incubated with fluorescent secondary antibodies (1:500, A48282, Invitrogen & 1:500, A48286, Invitrogen) and nuclei stained using Hoechst 33342 (1:1,000, Sigma-Aldrich). TUNEL assay (UE-T6013S) was performed to recognize the apoptotic nuclei in paraffin-embedded tissue sections.

Single-cell RNA-sequencing (scRNA-seq) analysis

The single-cell sequencing data comes from the Gene Expression Omnibus (GEO) database, and the number is GSE150327. The data was analyzed using Seurat R package.

Organoid culture and transplantation

Salivary gland samples from *Sox9creER, Rosa-tdTomato* mice were used for isolation and development of ex vivo organoid culture. After washed gently in cold PBS, tissues were cut into approximately 1-mm pieces and washed again with cold PBS. Clean tissue was then incubated in Type IV Collagenase for 30 minutes with shaking from time to time in a 37℃ thermostat. Then the pieces were passed through 70-μm filters (BD Biosciences) and centrifuged at 270g for 5 min at 4°C. Precipitate was resuspended in 1 mL cold DMEM-F12(C11330500BT-1) and centrifugated at 200×g for 5 min. Precipitate were resuspended in cold Matrigel (Corning #356231) and cold media in a 50:50 ratio. Then plant the mixture in a 24-well plate and place it in a 37 ℃ incubator for 15 minutes to solidify the Matrigel. Finally, stem cell culture media was added from the side of the well. For organoid transplantation, 100–150 salivary gland organoid were collected and transplanted into wild type mice exposed to neck irradiation. Samples were collected one month after transplantation.

Statistical Analysis

Positive signals are counted with ImageJ. All statistical analyses were performed using GraphPad Prism 8.0 software. Quantity results were reported as mean ± standard deviation (S.D.) of three or more independent experiments.

Declarations

Ethics Statement

All animal experiments and procedures were approved by sun yat-sen University Institutional Animal Care and Use Committee (IACUC) and complied with the guidelines for the use and care of laboratory animals.

Consent for publication

Not applicable

Availability of data and materials

The single-cell RNA-seq data analysed during the current study is available at the NCBI's Gene Expression Omnibus (GEO) data repository with the accession ID GSE150327.
https://www.ncbi.nlm.nih.gov/search/all/?term=GSE150327

Competing interests

The authors declared no potential conflicts of interest.

Funding

This paper was supported by the KEY PROJECT (BWS18J008), Natural Science Foundation of China (No. 81974443) and Natural Science Foundation of Guangdong Province (No. 2018A030313176).

Author Contributions

DC, CW, YB and TJL conceived and designed this project. XX and GX conducted experiments and interpreted results of experiments. MZ, XJX and SC drafted paper, edited and revised manuscript. All authors read and approved the final manuscript.

Acknowledgments

We thank Jackson Laboratory for providing transgenic mice. We appreciate Rongsong Ling for professional advice on the data analysis.

References

1. Chow LQM. Head and Neck Cancer. N Engl J Med. 2020;382(1):60–72.
2. Vissink A, Mitchell JB, Baum BJ, Limesand KH, Jensen SB, Fox PC, et al. Clinical management of salivary gland hypofunction and xerostomia in head-and-neck cancer patients: successes and barriers. Int J Radiat Oncol Biol Phys. 2010;78(4):983–91.
3. Emami B, Lyman J, Brown A, Coia L, Goitein M, Munzenrider JE, et al. Tolerance of normal tissue to therapeutic irradiation. Int J Radiat Oncol Biol Phys. 1991;21(1):109–22.
4. Lombaert IM, Brunsting JF, Wierenga PK, Faber H, Stokman MA, Kok T, et al. Rescue of salivary gland function after stem cell transplantation in irradiated glands. PLoS One. 2008;3(4):e2063.
5. Ogawa M, Oshima M, Imamura A, Sekine Y, Ishida K, Yamashita K, et al. Functional salivary gland regeneration by transplantation of a bioengineered organ germ. Nat Commun. 2013;4:2498.
6. Pringle S, Maimets M, van der Zwaag M, Stokman MA, van Gosliga D, Zwart E, et al. Human Salivary Gland Stem Cells Functionally Restore Radiation Damaged Salivary Glands. Stem Cells. 2016;34(3):640–52.
7. Aure MH, Arany S, Ovitt CE. Salivary Glands: Stem Cells, Self-duplication, or Both? J Dent Res. 2015;94(11):1502–7.
8. Song EC, Min S, Oyelakin A, Smalley K, Bard JE, Liao L, et al. Genetic and scRNA-seq Analysis Reveals Distinct Cell Populations that Contribute to Salivary Gland Development and Maintenance. Sci Rep. 2018;8(1):14043.
9. Knox SM, Lombaert IM, Reed X, Vitale-Cross L, Gutkind JS, Hoffman MP. Parasympathetic innervation maintains epithelial progenitor cells during salivary organogenesis. Science. 2010;329(5999):1645–7.
10. Lombaert IM, Abrams SR, Li L, Eswarakumar VP, Sethi AJ, Witt RL, et al. Combined KIT and FGFR2b signaling regulates epithelial progenitor expansion during organogenesis. Stem Cell Reports. 2013;1(6):604–19.
11. Kwak M, Ghazizadeh S. Analysis of histone H2BGFP retention in mouse submandibular gland reveals actively dividing stem cell populations. Stem Cells Dev. 2015;24(5):565–74.

12. Kwak M, Alston N, Ghazizadeh S. Identification of Stem Cells in the Secretory Complex of Salivary Glands. J Dent Res. 2016;95(7):776–83.
13. Chatzeli L, Gaete M, Tucker AS. Fgf10 and Sox9 are essential for the establishment of distal progenitor cells during mouse salivary gland development. Development. 2017;144(12):2294–305.
14. Dutta D, Heo I, Clevers H. Disease Modeling in Stem Cell-Derived 3D Organoid Systems. Trends Mol Med. 2017;23(5):393–410.
15. Schunk SJ, Floege J, Fliser D, Speer T. WNT-beta-catenin signalling - a versatile player in kidney injury and repair. Nat Rev Nephrol. 2021;17(3):172–84.
16. Siegel RL, Miller KD, Jemal A. Cancer statistics. 2015. CA Cancer J Clin. 2015;65(1):5–29.
17. Furuyama K, Kawaguchi Y, Akiyama H, Horiguchi M, Kodama S, Kuhara T, et al. Continuous cell supply from a Sox9-expressing progenitor zone in adult liver, exocrine pancreas and intestine. Nat Genet. 2011;43(1):34–41.
18. Chang DR, Martinez Alanis D, Miller RK, Ji H, Akiyama H, McCrea PD, et al. Lung epithelial branching program antagonizes alveolar differentiation. Proc Natl Acad Sci U S A. 2013;110(45):18042–51.
19. Rockich BE, Hrycaj SM, Shih HP, Nagy MS, Ferguson MA, Kopp JL, et al. Sox9 plays multiple roles in the lung epithelium during branching morphogenesis. Proc Natl Acad Sci U S A. 2013;110(47):E4456-64.
20. Malhotra GK, Zhao X, Edwards E, Kopp JL, Naramura M, Sander M, et al. The role of Sox9 in mouse mammary gland development and maintenance of mammary stem and luminal progenitor cells. BMC Dev Biol. 2014;14:47.
21. Zhao CM, Hayakawa Y, Kodama Y, Muthupalani S, Westphalen CB, Andersen GT, et al. Denervation suppresses gastric tumorigenesis. Sci Transl Med. 2014;6(250):250ra115.
22. Seymour PA, Freude KK, Tran MN, Mayes EE, Jensen J, Kist R, et al. SOX9 is required for maintenance of the pancreatic progenitor cell pool. Proc Natl Acad Sci U S A. 2007;104(6):1865–70.
23. Nanduri LS, Lombaert IM, van der Zwaag M, Faber H, Brunsting JF, van Os RP, et al. Salisphere derived c-Kit + cell transplantation restores tissue homeostasis in irradiated salivary gland. Radiother Oncol. 2013;108(3):458–63.
24. Nanduri LS, Baanstra M, Faber H, Rocchi C, Zwart E, de Haan G, et al. Purification and ex vivo expansion of fully functional salivary gland stem cells. Stem Cell Reports. 2014;3(6):957–64.
25. Tsuchida T, Murata S, Matsuki K, Mori A, Matsuo M, Mikami S, et al. The Regenerative Effect of Portal Vein Injection of Liver Organoids by Retrorsine/Partial Hepatectomy in Rats. Int J Mol Sci. 2019;21(1).
26. Sampaziotis F, Justin AW, Tysoe OC, Sawiak S, Godfrey EM, Upponi SS, et al. Reconstruction of the mouse extrahepatic biliary tree using primary human extrahepatic cholangiocyte organoids. Nat Med. 2017;23(8):954–63.
27. Ramsden CM, Powner MB, Carr AJ, Smart MJ, da Cruz L, Coffey PJ. Stem cells in retinal regeneration: past, present and future. Development. 2013;140(12):2576–85.

28. Agopian VG, Chen DC, Avansino JR, Stelzner M. Intestinal stem cell organoid transplantation generates neomucosa in dogs. J Gastrointest Surg. 2009;13(5):971–82.

Figures

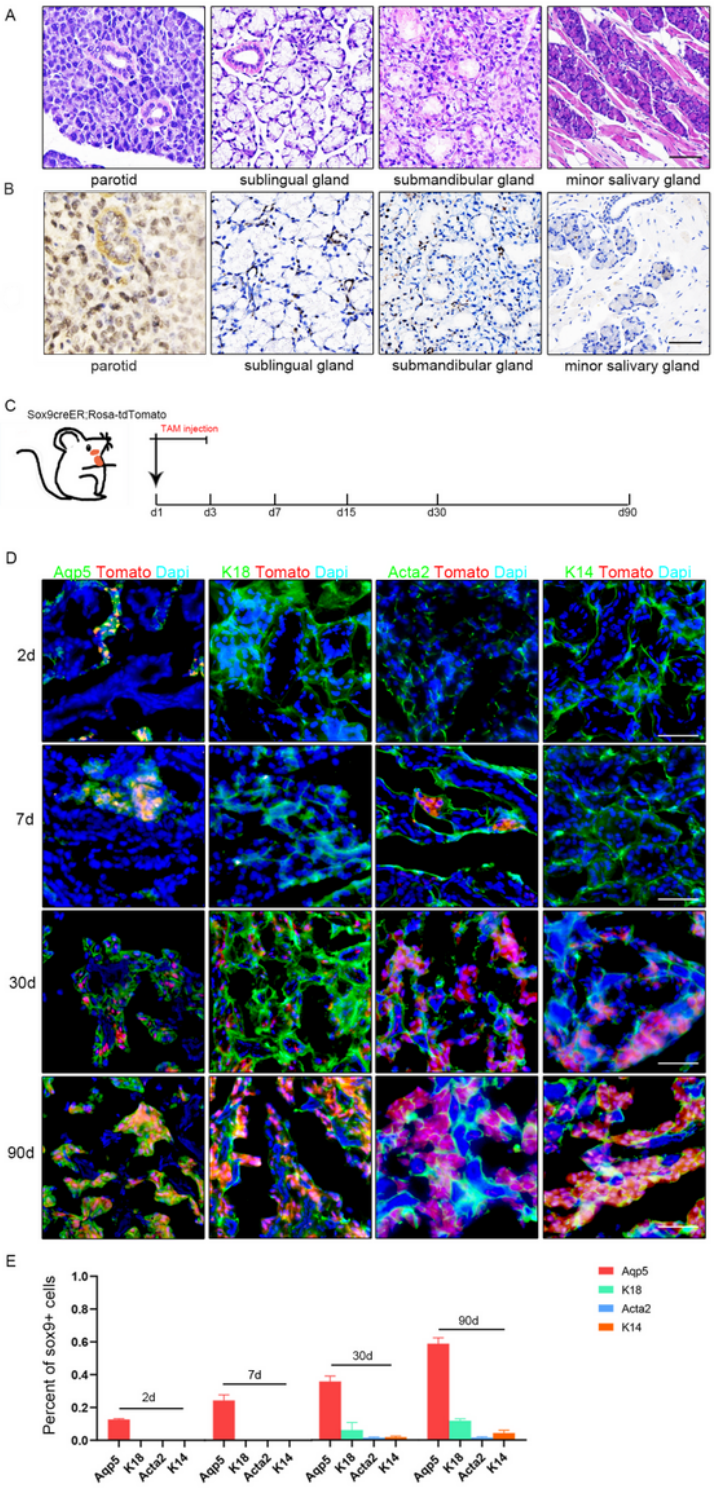

Figure 1

A. H&E staining images of normal mice salivary glands includes parotid glands, sublingual glands, submandibular glands and minor salivary glands. Scale bar:50um B. Images of normal mice minor salivary glands, parotid glands, sublingual glands, and submandibular glands immunostained for Sox9. Scale bar:50um C. Sox9creER; Rosa-tdTomato mice were injected with tamoxifen for three days. Collect submandibular gland at 1st,3rd,7th,15th,30th,60th,90th. D. Representative images of Sox9 lineage-traced submandibular gland under homeostasis condition. At 2th,7th,30th,90th, immunostaining for acinar markers (Aqp5), ductal cell markers(K18), myoepithelial marker (Acta2) and basal cell marker (K14) respectively. Nuclei were stained with Dapi (blue) Scale bar:50um E. Aqp5+Sox9+cells, K18+Sox9+cells, Acta2+Sox9+ cells, K14+Sox9+ cells account for the percentage of total cells at 2nd,7th,30th,90th

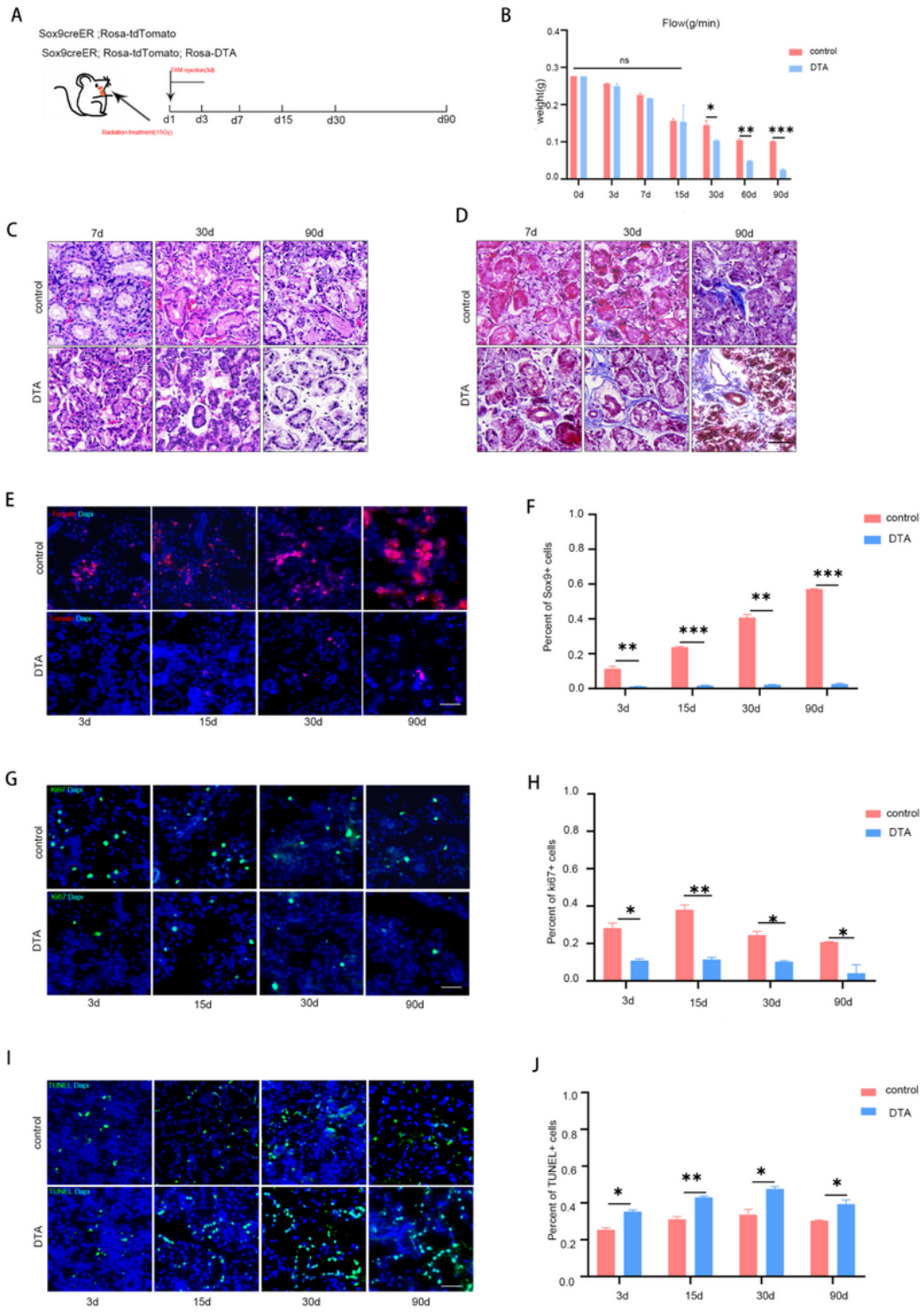

Figure 2

A. After 15Gy radiation, Sox9creER; Rosa-tdTomato mice (control group) and Sox9creER; Rosa-DTA (experimental group) were injected with tamoxifen for three days. (n = 3 per group). Collect submandibular gland tissue at 1st, 3rd, 15th, 30th, 90th. B. Measure the salivary gland flow rate of the two groups of mice at different time points. Data were analyzed using a multiple-tests or one-per row analysis. *p<0.05, **p<0.01, ***p<0.001 C. D Representative images of H&E staining and Masson's

trichrome staining in the two groups at different time points. Scale bar:50um E. G and I Immunostaining of Sox9+ cell-driven lineage tracing, Ki67 and TUNEL in Sox9creER; RosaDTA mice and control group. Scale bar, 50 μm. F. H and J Immunostaining scores of Sox9, Ki67 and TUNEL were counted respectively. ∗p<0.05, ∗∗p<0.01, and ∗∗∗p<0.001.

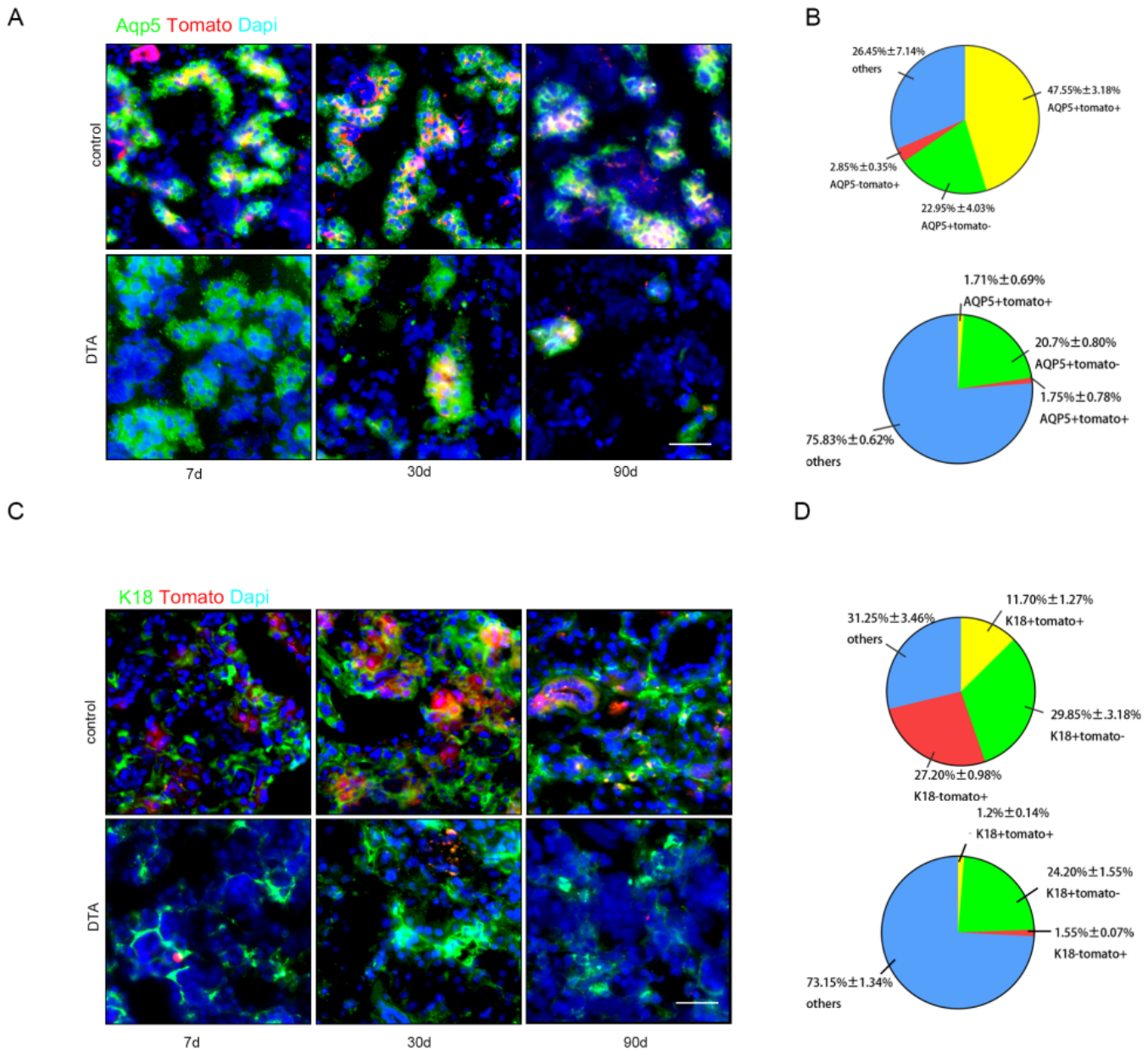

Figure 3

A. Representative immunofluorescence image of co-staining with acinar markers (Aqp5) after radiation damage at different time point between control and DTA groups. Scale bar, 50μm B. Quantification analyses of Aqp5+Tomato- cells, Aqp5+Tomato+ cells, Aqp5-Tomato+cells, other cells at the 90th day between control and DTA groups. C. Representative immunofluorescence image of co-staining with ductal cell markers (K18) after radiation damage at different time point between control and DTA groups.

Scale bar, 50μm D. Quantification analyses of K18+Tomato- cells, K18+Tomato+ cells, K18-Tomato+cells, other cells at the 90th day between control and DTA groups.

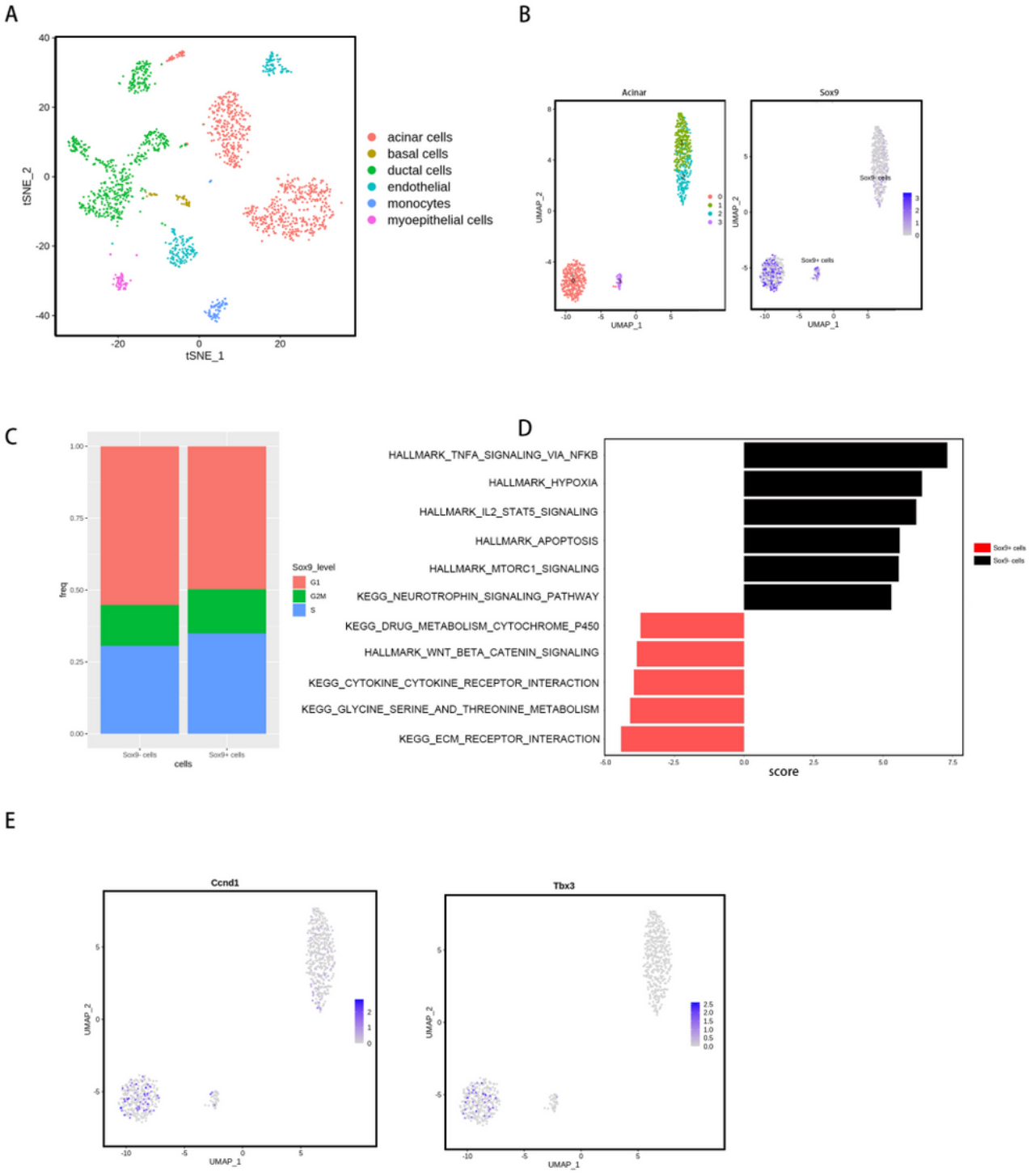

Figure 4

A. t-SNE plot of normal mice salivary gland cells reveal consistent clusters. Clusters are assigned to indicated cell types by differentially expressed genes. B. UMAP plots that describe clustering results based on the Sox9 expression level of acinar cells C. Cell cycle score between Sox9+ cells clusters and

Sox9-cells cluster. D. KEGG enrichment analysis indicated the statistically significant enriched pathways between Sox9+ cells clusters and Sox9-cells cluster. E. FeaturePlots that describe the expression level of Ccnd1, Tbx3, which are the target of Wnt/β-catenin pathway, between Sox9+ cells cluster and sox9-cells cluster.

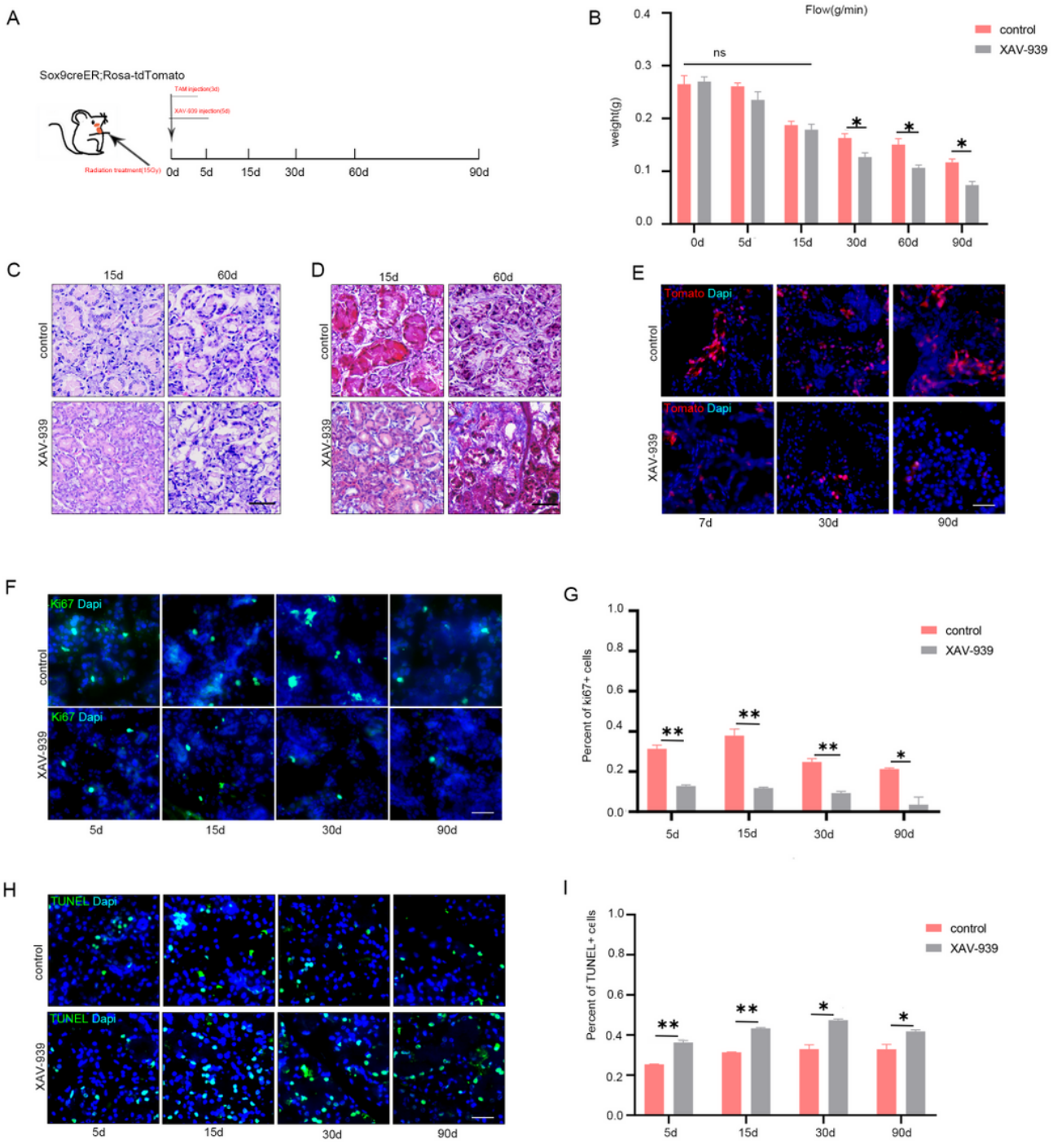

Figure 5

A. After 15Gy radiation, Sox9creER; Rosa-tdTomato mice were injected with tamoxifen and XAV-939 for three days and five days respectively (n = 3 per group). Collect submandibular gland at 1st, 3rd, 15th,

30th, 60th, 90th. B. Measure the salivary gland flow rate of the two groups (control and XAV-939 group) of mice at different time points. Data were analyzed using a multiple-tests or one-per row analysis. *p<0.05, **p<0.01, ***p<0.001 C. Representative images of H&E staining in the two groups at different time points. Scale bar:50um D. Representative images of Masson's trichrome staining in the two groups at different time points. Scale bar:50um E. Immunostaining images of Sox9+ cell-driven lineage tracing in mice injected with XAV-939 and control group. Scale bar, 50 μm. F. H Immunostaining of Ki67 and TUNEL in mice injected with XAV-939 and control group. Scale bar, 50 μm. G. I Immunostaining scores of Ki67 and TUNEL were counted respectively. ∗p<0.05, ∗∗p<0.01, and ∗∗∗p<0.001.

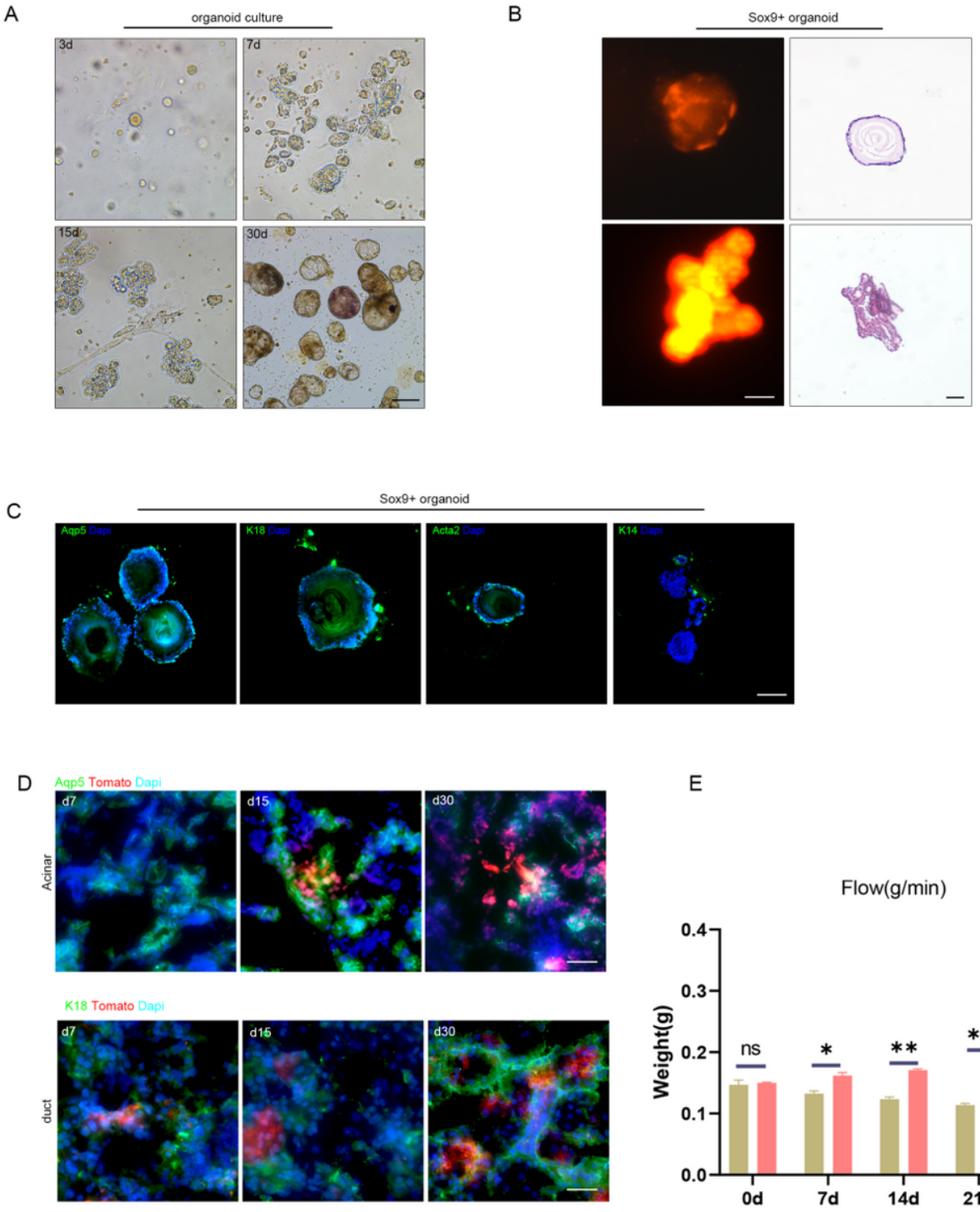

Figure 6

A. Representative brightfield images of Sox9+ organoids development. Scale bar, 50 μm. B. Representative fluorescence of Sox9+ organoids with different forms. Scale bar, 100 μm. H&E images of Sox9+ organoids with different forms. Scale bar, 50 μm C. Representative images of differentiated Sox9+ organoids expressing acinar cell marker (Aqp5), ductal cell marker (K18), myoepithelial marker (Acta2) and basal cell marker (K14). Scale bar, 50 μm. D. Representative fluorescence images of salivary gland after transplant of Sox9+ organoids. Scale bar, 50 μm. E. Measure the salivary gland flow rate of the two groups (control and organoid transplantation groups) of mice at different time points(Start timing one month after injury). Data were analyzed using a multiple-tests or one-per row analysis. *$p<0.05$, **$p<0.01$, ***$p<0.001$